Nuclear Engineering and Technology xxx (xxxx) xxx

Contents lists available at ScienceDirect

Nuclear Engineering and Technology

journal homepage: www.elsevier.com/locate/net

Original Article

Continuous beta monitoring technology for uncontrolled radiological release in underwater using integrated beta and gamma detection system

Woo Nyun Choi [a,1], Seungbin Yoon [b,1], Hyeonmin Lee [b], Hee Reyoung Kim [b,*]

[a] Nuclear Power Plant Business Group, Doosan Enerbility, 22 DoosanVolvo-ro, Seongsan-gu, Changwon, Gyeongnam, 51711, Republic of Korea
[b] Department of Nuclear Engineering, Ulsan National Institute of Science and Technology (UNIST), 50 UNIST-gil, Ulju-gun, Ulsan, 44919, Republic of Korea

ARTICLE INFO

Keywords:
Beta and gamma detection system
In-situ measurement
Continuous monitoring
Water sample

ABSTRACT

A monitoring system capable of in-situ beta detection has been developed to address the potential risks associated with radioactive releases from nuclear sites. Although releases are controlled within permissible limits and follow strict protocols to minimize environmental and public health impacts, incidents of uncontrolled releases due to human or mechanical failures have occurred, resulting in contamination of underground water sources. To improve response capabilities, transitioning from traditional sample-based monitoring to real-time monitoring of underground water is crucial. The system utilized an NaI(Tl) detector for gamma nuclides and two plastic scintillation detectors for beta nuclides. Beta detection was facilitated through a coincidence method involving the two plastic scintillators, with any influence from gamma radiation effectively mitigated using data from the NaI(Tl) detector. This configuration ensured accurate measurement of beta radiation by removing gamma contributions from the coincidence counts. The system, which was evaluated using detection experiments for beta nuclides ^{3}H and ^{90}Sr, achieved a minimum detectable activity that satisfied the criteria for restricting the intake, distribution, or consumption of ^{90}Sr and ^{3}H to 0.1 and 100 Bq/g, respectively, within 20 min.

1. Introduction

Radioactive substances produced during the operations of nuclear facilities such as nuclear power plants (NPPs) are released into the environment in accordance with legal limits. These releases, although minor, are meticulously planned to follow the operational protocols outlined in the technical manuals of NPPs. The radioactivity levels of these releases are controlled to minimize adverse impacts on neighboring communities and the environment, thereby safeguarding public health by maintaining radiation doses at the lowest practicable levels. Despite these precautions, uncontrolled releases may still occur. Historical instances in the U.S. have demonstrated that uncontrolled releases can occur owing to system leaks or operator errors during both the decommissioning and operational phases of NPPs, resulting in radioactive contamination of groundwater [1,2]. In contrast to planned releases, such uncontrolled discharges bypass established management protocols, introducing radioactive materials into the environment in an unchecked and unregulated manner. Therefore, NPP operators must proactively address these risks, recognizing potential causes and challenges in ensuring prevention. This highlights the importance of promptly identifying any unplanned releases to facilitate swift remedial action.

In compliance with Notice No. 2017-17 from the Korea Nuclear Safety and Security Commission, which mandates regulations on environmental radiological surveillance and environmental radiological impact assessments near nuclear sites, the environmental radioactivity of areas surrounding Korean NPPs is rigorously evaluated [3]. Water samples from rain, surface water, and groundwater are collected monthly for environmental radiological surveillance and analyzed for radionuclides such as gross-beta, tritium, and gamma [4]. Owing to the short range of low-energy beta radionuclides, these analyses typically require the use of liquid scintillation counters (LSC), which necessitate a pre-treatment procedure and extended analysis times, thus making in-situ measurement unfeasible [4]. This limitation impedes rapid responses to uncontrolled releases. Consequently, a system was developed for in-situ beta measurements [5,6]. However, additional research is necessary to determine if gamma nuclides are included in water samples.

In this study, a monitoring system is developed to rapidly detect groundwater contamination caused by beta radiation due to

* Corresponding author.
E-mail address: kimhr@unist.ac.kr (H.R. Kim).
[1] These authors contributed equally to this work.

https://doi.org/10.1016/j.net.2024.10.010
Received 1 August 2024; Received in revised form 7 October 2024; Accepted 8 October 2024
Available online 9 October 2024

uncontrolled releases, which may occur during both the decommissioning and operational phases of NPPs. To eliminate the influence of gamma radiation present in groundwater and accurately measure beta radionuclides in real-time, the system integrates plastic scintillators and an NaI(Tl) scintillator. The real-time data provided by this system enables rapid detection of groundwater beta contamination resulting from uncontrolled releases, thus facilitating prompt corrective actions to minimize environmental impact.

2. Material and methods

2.1. Minimum detectable activity (MDA)

MDA is a critical indicator of the performance of the detection system, signifying the minimum amount of nuclides that can be analyzed reliably [7,8]. The MDA determination in this study employs the method developed by Currie to assess the activity of unknown samples. Defined by Currie at a 95 % confidence level, the MDA is calculated using Equation (1) [9], which considers factors such as background counts, detection efficiency, and sample mass:

$$\mathrm{MDA} = \frac{2.71 + 4.65\sqrt{r_b \times T}}{T \bullet m \bullet \varepsilon \bullet K} \left[\frac{\mathrm{Bq}}{\mathrm{g}}\right], \quad (1)$$

where.

r_b = background count rate (cps),
T = sample and background counting time (s),
m = sample mass (g),
ε = detection efficiency,
K = recovery factor.

Optimizing the detection efficiency and sample mass, along with minimizing the background counts, is crucial for reducing the MDA.

2.2. Configuration of the monitoring system

Fig. 1 shows the overall configuration of the continuous beta monitoring system. The monitoring system is primarily composed of three main components: the support structure, the detection system, and the dark box. The support structure stores water samples and facilitates its contact with the detection system. The detection system includes the detectors for beta monitoring and the necessary circuitry. The dark box is designed to prevent interference from ambient light. The detectors are located inside the dark box, while other electronic circuitry is positioned in the lower section of the dark box. As shown in Fig. 1, hose connections are made on both sides of the dark box and support structure. Groundwater is pumped from outside the dark box, and the collected groundwater flows into the support structure through the hose. Once the support structure is completely filled with water, the pump stops, and the measurement is performed.

2.2.1. Support structure for the sample and plastic scintillators

Previous research utilized a detection system based on a plastic scintillator, an organic scintillator recognized for its durability in direct contact with water and its ability to detect beta nuclides [5,6]. However, in basic research, when gamma nuclides are present in water samples, beta detection can be overestimated using conventional systems. To address this, a detection system has been designed, which utilizes an NaI (Tl) scintillator with aluminum shielding to prevent beta nuclide interaction at the detection part. A reflector encloses the scintillator, which includes both the sample and the support structure for the plastic scintillators.

The support structure for the sample and plastic scintillators is designed in SolidWorks [10]. The detection unit is a cube with a volume of 216 cm^3 (each side measuring 6 cm) and a thickness of 5 mm. Plastic scintillators, each with a diameter of 5 cm, are inserted into the front and rear with a depth of 3 mm. A hole with a diameter of 44 mm supports the plastic scintillator, creating a 2 mm thick gap with a length of 3 mm. Reducing the length of this gap increases the contact area between the plastic scintillator and water, thereby enhancing measurement efficiency. This design also considers mechanical safety under internal water pressure. A protrusion with an outer diameter of 10 mm and an inner diameter of 8 mm allows for water flow, while the flat modeling of the remaining side facilitates measurements using a NaI(Tl) detector. The actual appearance of the sample and plastic scintillator support structure is produced using 3D printing technology.

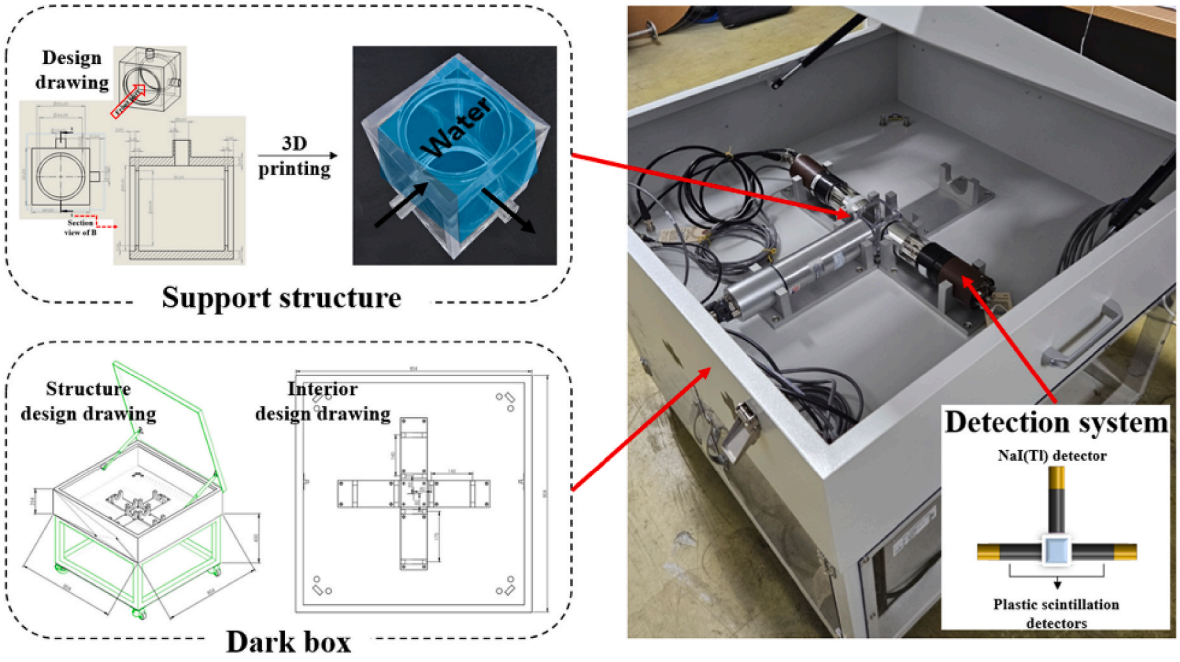

Fig. 1. Overall configuration of the continuous beta monitoring system.

2.2.2. Detection system

Fig. 2 presents a flowchart of the method for integrated beta and gamma detection. Initially, for a water sample contaminated with both beta and gamma nuclides, gamma photopeak counts are measured using a NaI(Tl) scintillator, and gamma activity is analyzed based on these counts. Subsequently, the coincidence counts, which include both beta and gamma, are assessed using plastic scintillators. An analysis of the impact of gamma nuclides on the counts from plastic scintillators allows for an evaluation of gamma's influence on the coincidence counts, informed by the gamma nuclide data obtained from the NaI(Tl) scintillator. After adjusting for the effects of gamma nuclides, background counts are further subtracted to isolate the coincidence counts attributable to gross-beta. These gross-beta coincidence counts are then used to calculate both the detection efficiency and MDA for gross-beta.

In the context of gross-beta detection, the process involves deriving coincidence counts. Fig. 2 shows the circuit sequence diagram of the integrated beta and gamma detection system. To detect incident radiation, a high-voltage power supply (556, ORTEC) applies an operating voltage to the photomultiplier tube (PMT) [11]. The two output signals from the PMT are simultaneously amplified using a dual amplifier (855, ORTEC) [12]. These amplified signals are then processed through a timing single-channel analyzer (SCA; 551, ORTEC) and a time-to-amplitude converter (567, ORTEC) employing a coincidence method designed to minimize background effects [13–15]. The signal obtained via this coincidence method is digitized using a multichannel analyzer (EASY-MCA 2K, ORTEC) [16]. This setup also facilitates the acquisition of the energy spectrum for gamma nuclides, employing the same high-voltage power supply, amplifier, and multichannel analyzer.

2.2.3. Dark box

In beta and gamma measurements, interference from ambient light must be prevented. To achieve this, a dark box has been designed and manufactured to completely block light and securely mount the scintillator support structure and the detector that measures the water sample. This setup ensures that the condition of the detection components within the dark box can be maintained without the influence of external light.

This study employs two PMT R878s and one NaI(Tl) detector within the dark box. However, the dark box is designed to accommodate up to four detectors. This allows for considerable flexibility in conducting measurements and ensures ample space within the unit. The frame of the dark box is constructed from S45C steel with a thickness of 2 mm.

The internal layout of the dark box features four corners equipped with a BNC adapter, a 9-pin D-sub gender changer, and an SHV adapter. These components facilitate the connection of the detectors inside the dark box to external measurement systems. Special consideration is given to the design of the lower part of the dark box to create adequate space for these adapters and gender changers, thus simplifying connectivity.

The detector support structure within the dark box is precisely designed to match the dimensions of the PMT R878 and NaI detectors. This ensures that the detectors can be securely fixed, eliminating any risk of movement during the radiation monitoring process.

2.3. Optimization of gross-beta detection in water using real-time measurement

Three major radionuclides in the groundwater are used to test the monitoring system for gross-beta detection. The beta sources include ^{3}H and ^{90}Sr, with ^{137}Cs serving as the gamma source. These radionuclides are selected based on their prevalence in documented cases of

Table 1
Information on beta and gamma sources.

	^{3}H	$^{90}Sr/^{90}Y$	^{137}Cs
Initial radioactivity [Bq]	1.00E+05	3.71E+03/ 3.71E+03	3.67E+03
Mass of total source [g]	20.00	5.04	5.00
Date of production	210726	230803	230803
Activity concentration on production date [Bq/g]	5.01E+03	7.36E+02/ 7.36E+02	7.35E+02
Volume of support structure [g]	131.08		
Amount of liquid source injected [g]	4	1	
	6	1.5	
	8	2	
Radioactivity of sample [Bq]	1.77E+04	1.46E+03	7.31E+02
	2.65E+04	2.20E+03	1.10E+03
	3.54E+04	2.94E+03	1.46E+03
Activity concentration on measurement date [Bq/g]	1.35E+02	1.12E+01	5.58E+00
	2.02E+02	1.68E+01	8.37E+00
	2.70E+02	2.24E+01	1.12E+01

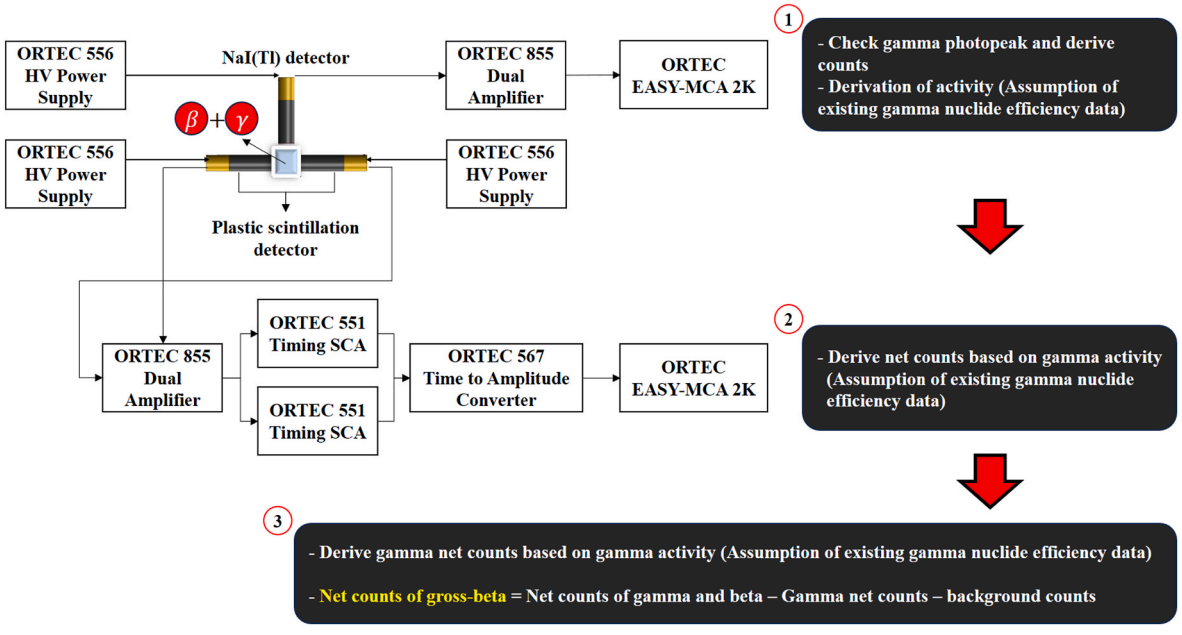

Fig. 2. Circuit sequence diagram and flowchart of the integrated beta and gamma detection method.

groundwater contamination from uncontrolled releases in the U.S [17].

Table 1 details the initial radioactivity, mass, production date, and activity concentration on both production and measurement dates for the beta (^{3}H, ^{90}Sr) and gamma (^{137}Cs) unsealed sources used in this experiment. The production dates are as follows: 03-August-2023, 12:00 p.m. EST for ^{90}Sr and ^{137}Cs, and 26-July-2021, 12:00 p.m. EST for ^{3}H. The ^{90}Sr source was certified only for radioactivity of ^{90}Sr. By the measurement date, enough time has passed since the production date, allowing the parent ^{90}Sr to reach radioactive equilibrium with the daughter ^{90}Y. All measurements derived from these sources are corrected for radioactive decay from the production date to the measurement date. Samples at three different activity concentrations are prepared for each source. The full-energy peak efficiency (FEPE) for ^{137}Cs using NaI(Tl) scintillators and the detection efficiency for ^{137}Cs using plastic scintillators are determined. The reliability of the detection system is validated by comparing the detection efficiencies at different activities of ^{137}Cs for each scintillator. Detection efficiencies are determined by measuring coincidence counts for ^{90}Sr at varying activities using plastic scintillators. The system's reliability is confirmed through comparisons of the derived detection efficiencies.

To verify the functionality of the monitoring system, experiments are conducted using mixed sources of beta and gamma. Table 2 provides the information for these beta and gamma mixed sources of ^{90}Sr and ^{137}Cs nuclides. Detection efficiency for the ^{90}Sr beta source is derived based on detection efficiency data from experiments with single-source samples. The detection efficiency of ^{90}Sr obtained from ^{90}Sr + ^{137}Cs mixed samples is compared with the detection efficiency observed when only ^{90}Sr is present, thus confirming the reliability of the detection system. From the established detection efficiency and the measured coincidence counts for ^{90}Sr, the MDA value for ^{90}Sr is calculated.

An experiment aimed at detecting ^{3}H, with its maximum energy of 18.6 keV, is also conducted using the developed monitoring system. The ^{3}H detection experiments involve samples with radioactivities of 1.77E+04, 2.65E+04, and 3.54E+04 Bq, as listed in Table 1. The coincidence counts over 24 h of measurement time using plastic scintillators for ^{3}H are determined, and the detection efficiency is calculated by subtracting the coincidence counts measured over 24 h for distilled water.

2.4. Derivation of KCl efficiency for gross-beta measurement

In the context of calibrating environmental radiation monitoring systems for gross-beta measurements, a key challenge is the unknown nature of the nuclides present in environmental samples. Generally, natural radionuclides in such samples emit a maximum beta energy of approximately 1 MeV. Accordingly, nuclides emitting this energy level are typically utilized as standard sources for calibration. Among these, ^{40}K is commonly chosen owing to its long half-life and stability, making it easy to handle in a standard chemistry laboratory setting. Notably, ^{40}K is naturally present in KCl and is exempt from radiation regulations [18]. Similar to the method by which gross-beta is measured in low-level alpha/beta counters, this monitoring system employs KCl to calibrate counting efficiency.

To assess the overall counting efficiency, measurements are conducted on manufactured KCl standard samples for 60 min each. The natural abundance ratio of ^{40}K in potassium is 0.0117 %, allowing for the calculation of radioactivity in 1 mg of KCl to be approximately 14.78 mBq, or 0.015 disintegrations per second (dps). Counting efficiency is thus determined using Equation (2).:

$$\varepsilon = \frac{r_N}{0.015 \times W} \times 100 \quad (2)$$

where.

r_N = net count rate of the KCl sample (cps),
W = weight of KCl (mg).

Measurements to derive efficiencies are performed on six samples, as detailed in Table 3.

3. Results and discussion

3.1. Results of underwater gamma full-energy peak efficiency and detection efficiency based on coincidence counts

Table 4 presents the net area counts of the full peak, background counts, and FEPE according to changes in the radioactivity of ^{137}Cs in the NaI(Tl) detection part. The FEPE of the NaI(Tl) detection part for ^{137}Cs samples in water is determined to be 1.589 ± 0.0274 % at a 95 % confidence level (k = 2, where k is the coverage factor determining an approximate 95 % confidence level at the combined uncertainty). This value includes uncertainties arising from source radioactivity, full peak emission probability, and measurement counts. Fig. 3 (a) shows the linearity of the increase in net area counts of the full peak value in relation to the radioactivity of ^{137}Cs, with a coefficient of determination (R^2) of 1.

Table 5 outlines the coincidence net counts, coincidence net count rate, and detection efficiencies in response to changes in the radioactivity of the ^{137}Cs sample in the plastic scintillators based detection part. The uncertainty in detection efficiency is the combined uncertainty of the radioactivity uncertainty of the sources used in the experiment, volume uncertainty, and counting uncertainty of the measurement. The detection efficiency for the plastic scintillators based detection part for ^{137}Cs samples in water is determined to be 0.758 ± 0.0132 % (95 % confidence level, k = 2). Fig. 3 (b) shows the linearity of the increase in net coincidence counts according to the radioactivity of ^{137}Cs, with an R^2 value of 0.9999.

3.2. Results of underwater gross-beta detection efficiency based on coincidence counts

Table 6 presents the results for coincidence net counts, coincidence net count rate, and detection efficiencies according to changes in the radioactivity of ^{90}Sr in the plastic scintillators based detection part. The uncertainty in detection efficiency is the combined uncertainty of the radioactivity uncertainty of the sources used in the experiment, the volume uncertainty, and the counting uncertainty of the measurements. The detection efficiency for the plastic scintillators based detection part for ^{90}Sr samples in water is derived to be 2.535 ± 0.0304 % at a 95 % confidence level (k = 2). Fig. 3 (c) shows the linearity of the increase in net coincidence counts in response to the radioactivity of ^{90}Sr, with an R^2 value of 1.

Table 2
Information on beta and gamma mixed sources of ^{90}Sr + ^{137}Cs.

	Sample 1		Sample 2		Sample 3	
	^{90}Sr	^{137}Cs	^{90}Sr	^{137}Cs	^{90}Sr	^{137}Cs
Activity concentration on measurement date [Bq/g]	5.59E+00	5.58E+00	8.38E+00	4.18E+00	1.12E+01	2.79E+00
Radioactivity of sample [Bq]	7.32E+02	7.31E+02	1.10E+03	5.48E+02	1.46E+03	3.66E+02
Total radioactivity of sample [Bq]	1.46E+03		1.65E+03		1.89E+03	

Table 3
Information on KCl standard samples.

	Sample 1	Sample 2	Sample 3	Sample 4	Sample 5	Sample 6
Weight of KCl [g]	2	4	6	8	10	16
Radioactivity [Bq]	29.57	59.13	88.70	118.27	147.83	236.53
Measurement time [s]	3,600					

Table 4
NaI(Tl) detection part FEPE results for ^{137}Cs.

	^{137}Cs		
Radioactivity of sample [Bq]	731.43 ± 7.31	1,097.14 ± 10.97	1,468.10 ± 14.68
Measurement time [s]	1,800		
Net area of full peak [counts]	17,772 ± 162	26,626 ± 187	35,906 ± 211
Background counts	8,454 ± 92		
Emission probability	0.851 ± 0.001		
FEPE [%]	1.586 ± 0.022	1.584 ± 0.025	1.597 ± 0.024

FEPE, full-energy peak efficiency.

3.3. Results of underwater gross-beta detection efficiency and MDA derivation for beta and gamma mixed sources

Table 7 presents the net area counts of the full peak and FEPE derived by the NaI(Tl) detection part for samples mixed with ^{90}Sr and ^{137}Cs. The FEPEs for the NaI(Tl) detection part for the ^{137}Cs in these mixed samples are found to be 1.581 ± 0.028, 1.571 ± 0.022, and 1.583 ± 0.020 %, respectively, confirming consistency within the previously established range of 1.589 ± 0.0274 % (with a confidence level of 95 %, k = 2) as derived in Section 3.1.

Based on the detection efficiency of 0.758 ± 0.0132 % (with a confidence level of 95 %, k = 2) for the plastic scintillators based detection part for ^{137}Cs, as derived in Section 3.1, the coincidence net count rate for ^{137}Cs can be calculated using Equation (3). The coincidence net count rates for ^{137}Cs, shown in Table 8, are 365.64 ± 3.66, 548.45 ± 5.48, and 731.27 ± 3.31 Bq, in order of sample number, was calculated to be 2.77 ± 0.06, 4.16 ± 0.08, and 5.54 ± 0.11 cps, respectively, in order of sample number.

$$r_g - r_b = \frac{A \bullet \varepsilon}{100}, \tag{3}$$

where.

r_g = gross count rate (cps),
r_b = background count rate (cps),
A = activity (Bq),
ε = detection efficiency (%).

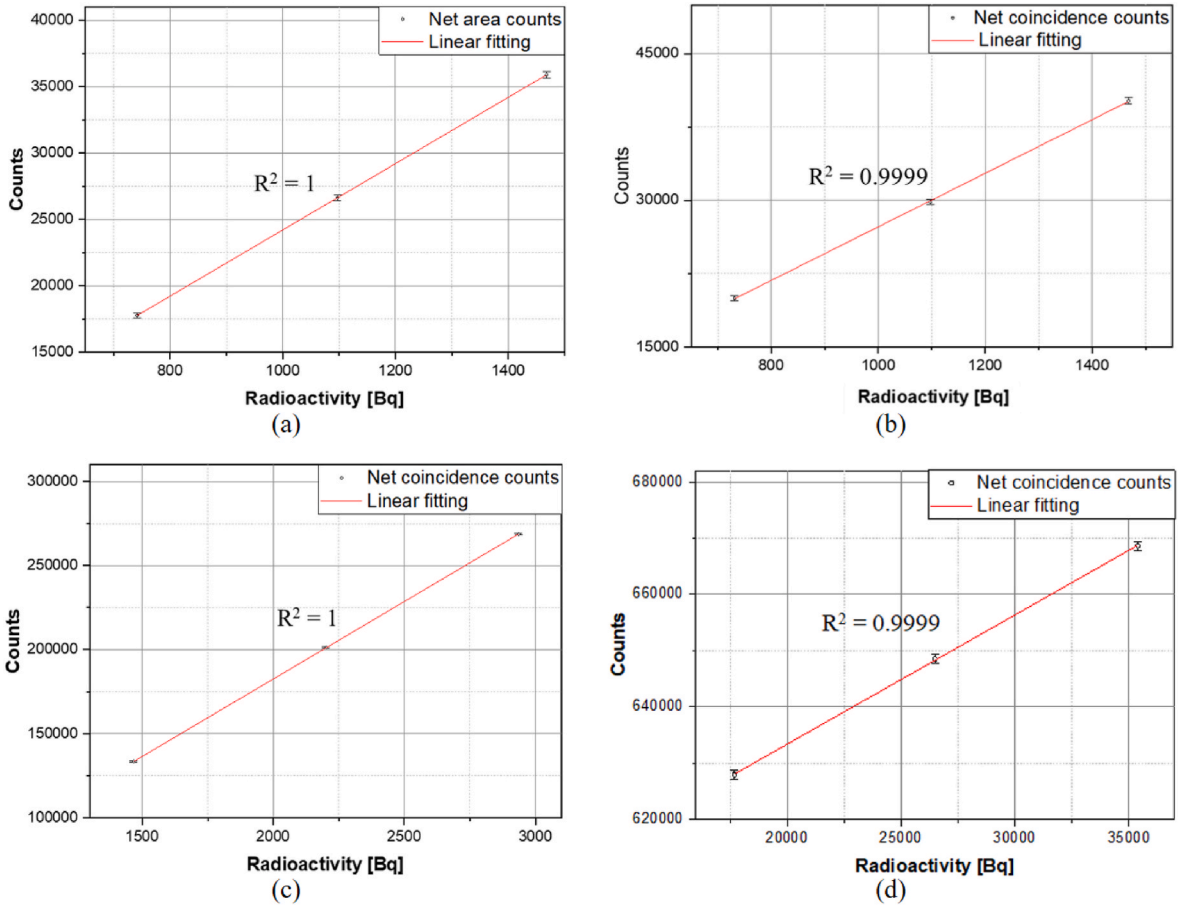

Fig. 3. Linearity fitting based on the detection part: (a) for ^{137}Cs based on NaI(Tl) scintillator; (b) for ^{137}Cs based on plastic scintillators; (c) for ^{90}Sr based on plastic scintillators; (d) for ^{3}H based on plastic scintillators.

Table 5
Plastic scintillators based detection part detection efficiency results for ^{137}Cs.

	^{137}Cs		
Radioactivity of sample [Bq]	731.43 ± 7.31	1,097.14 ± 10.97	1,468.10 ± 14.68
Background coincidence counts	27,256 ± 165		
^{137}Cs coincidence net counts	19,969 ± 273	29,826 ± 290	40,174 ± 308
Measurement time [s]	3,600		
^{137}Cs coincidence net count rate [cps]	5.55 ± 0.08	8.29 ± 0.08	11.16 ± 0.09
Detection efficiency [%]	0.758 ± 0.013	0.755 ± 0.011	0.760 ± 0.010

Table 6
Plastic scintillators based detection part detection efficiency results for ^{90}Sr.

	^{90}Sr		
Radioactivity of sample [Bq]	1,468.10 ± 14.68	2,202.14 ± 22.02	2,936.19 ± 29.36
Background coincidence counts	27,256 ± 165.09		
^{90}Sr coincidence net counts	133,353 ± 433	201,337 ± 505	268,629 ± 568
Measurement time [s]	3,600		
^{90}Sr coincidence net count rate [cps]	37.04 ± 0.08	55.93 ± 0.08	74.62 ± 0.09
Detection efficiency [%]	2.523 ± 0.027	2.540 ± 0.026	2.541 ± 0.026

Table 8 shows the background coincidence net counts, coincidence net counts, and ^{90}Sr detection efficiencies derived by the plastic scintillators-based detection part for water samples mixed with ^{90}Sr and ^{137}Cs. By subtracting the derived coincidence net count rate of ^{137}Cs from the total coincidence net count rate of the ^{90}Sr + ^{137}Cs sample (excluding the background count rate), the gross-beta coincidence count rate for ^{90}Sr is determined. The detection efficiencies for gross-beta of the plastic scintillator-based detection part are derived to be 2.572 ± 0.027, 2.586 ± 0.029, and 2.511 ± 0.033 %, in sample order. These values are confirmed to be within the detection efficiency range of 2.535 ± 0.0304 % (with a confidence level of 95 %, k = 2) for ^{90}Sr as derived in Section 3.2.

Assuming unknown radioactivity of the samples, the radioactivity values for ^{137}Cs and ^{90}Sr are calculated following the procedure outlined in Fig. 4. Table 9 compares these calculated radioactivity values with those obtained by measurement, along with their relative differences, which are derived using Equation (4):

$$\text{Relative difference} = \frac{\text{Activity by measurment} - \text{Activity by calculation}}{\text{Activity by measurment}} \times 100\ [\%] \quad (4)$$

The relative differences between the measured and calculated radioactivities ranged from 0.36 to 2.51 %, indicating consistency between the two methods for both ^{90}Sr and ^{137}Cs.

Table 10 presents the MDA values calculated for different measurement times based on the detection efficiency for the ^{90}Sr nuclide (2.535 ± 0.0304 %, with a confidence level of 95 %, k = 2) obtained through experiments. The uncertainty of MDA is the combined uncertainty of the background count, sample mass, and detection efficiency. To ensure conservative results, the highest values are considered, given the uncertainties.

Table 11 details the detection efficiency results for KCl samples used for deriving gross-beta. The detection efficiency of the plastic scintillators based detection part for KCl samples in water is calculated to be 1.564 ± 0.0917 % (with a confidence level of 95 %, k = 2).

When evaluating gross-beta radioactivity using detection efficiencies specific to different beta nuclides, the values can be underestimated or overestimated depending on which beta nuclides detection efficiency applied. For example, using the detection efficiency for ^{3}H, which is lower, tends to overestimate radioactivity, while using the higher detection efficiency for ^{90}Sr underestimates it. Therefore, the detection efficiency for KCl is derived following the same methodology used for gross-beta in a low-level alpha/beta counter, which allows for a derivation of gross-beta radioactivity.

3.4. Results of underwater ^{3}H detection efficiency and MDA derivation

Table 12 presents the background coincidence counts, ^{3}H coincidence net counts, ^{3}H coincidence net count rates, and detection efficiencies according to changes in the ^{3}H radioactivity of the plastic scintillators based detection part. The derived detection efficiencies for ^{3}H are found to be 2.64E−03 ± 8.22E−05, 2.66E−03 ± 6.28E−05, and 2.65E−03 ± 5.40E−05 %. Fig. 3 (d) shows the linearity of the increase

Table 7
NaI(Tl) detection part FEPE results for ^{137}Cs from ^{90}Sr + ^{137}Cs mixed samples.

Sample	1		2		3	
Radioactivity of sample [Bq]	^{90}Sr	^{137}Cs	^{90}Sr	^{137}Cs	^{90}Sr	^{137}Cs
	1,464.86 ± 14.65	365.64 ± 3.66	1,098.64 ± 10.99	548.45 ± 5.48	732.43 ± 7.32	731.27 ± 7.31
Measurement time [s]	3,600					
Net area of full peak [counts]	17,708 ± 227		26,400 ± 245		35,471 ± 263	
Background counts	16,900 ± 130					
Emission probability	0.851 ± 0.001					
FEPE [%]	1.581 ± 0.028		1.571 ± 0.022		1.583 ± 0.020	

FEPE, full-energy peak efficiency.

Table 8
Plastic scintillators based detection part detection efficiency results for ^{90}Sr from ^{90}Sr +^{137}Cs mixed samples.

Sample	1		2		3	
Radioactivity of sample [Bq]	^{90}Sr	^{137}Cs	^{90}Sr	^{137}Cs	^{90}Sr	^{137}Cs
	1,464.86 ± 14.65	365.64 ± 3.66	1,098.64 ± 10.99	548.45 ± 5.48	732.43 ± 7.32	731.27 ± 7.31
Measurement time [s]	3,600					
Background coincidence counts	28,980 ± 170					
^{90}Sr + ^{137}Cs coincidence net counts	145,633 ± 451		117,271 ± 419		86,157 ± 380	
^{137}Cs coincidence net count rate (calculated values) [cps]	2.77 ± 0.06		4.16 ± 0.08		5.54 ± 0.11	
^{90}Sr coincidence net count rate (calculated values) [cps]	37.68 ± 0.14		28.42 ± 0.14		18.39 ± 0.15	
^{90}Sr detection efficiency [%]	2.572 ± 0.027		2.586 ± 0.029		2.511 ± 0.033	

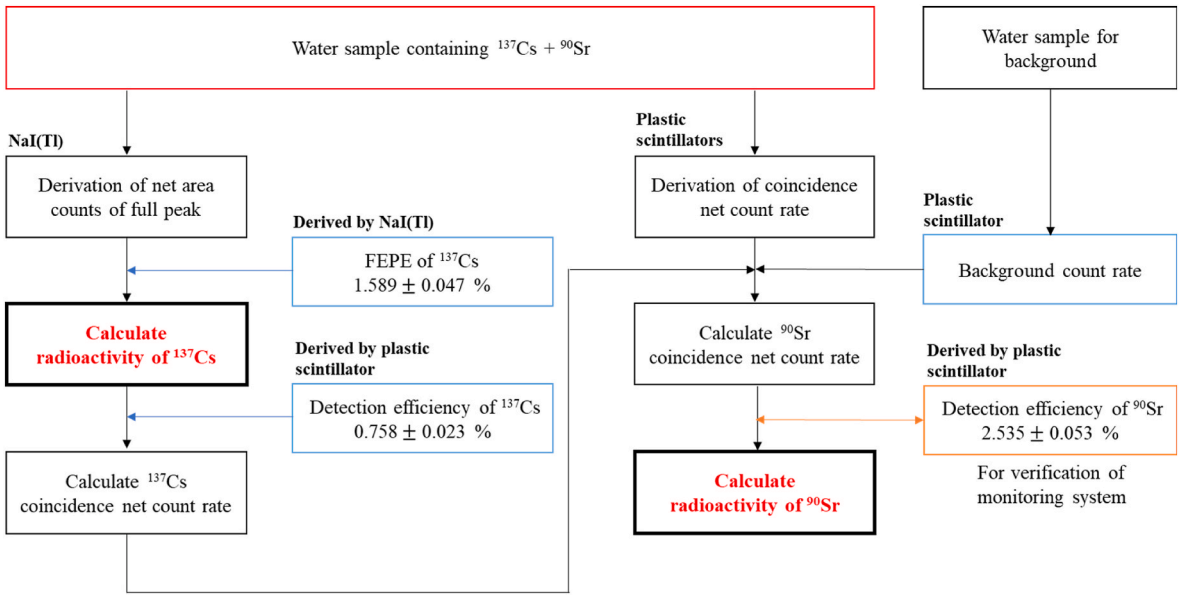

Fig. 4. Flowchart for deriving radioactivity from samples with unknown radioactivity.

Table 9
Values of radioactivity by measurement and calculation.

Sample	1		2		3	
	^{90}Sr	^{137}Cs	^{90}Sr	^{137}Cs	^{90}Sr	^{137}Cs
Radioactivity by measurement [Bq]	1,464.86 ± 14.65	365.64 ± 3.66	1,098.64 ± 10.99	548.45 ± 5.48	732.43 ± 7.32	731.27 ± 7.31
Radioactivity by calculation [Bq]	1487.03 ± 23.35	363.76 ± 8.40	1,122.86 ± 18.28	542.31 ± 11.58	726.21 ± 13.31	728.65 ± 14.82
Relative difference [%]	1.51 ± 1.88	− 0.51 ± 2.51	2.20 ± 1.94	− 1.12 ± 2.34	− 0.85 ± 2.07	− 0.36 ± 2.26

Table 10
MDA of ^{90}Sr and ^{3}H according to measurement time.

Time [min]	MDA of ^{90}Sr [Bq/g]	MDA of ^{3}H [Bq/g]
1	0.499	477.79
10	0.153	146.49
20	0.108	103.22
30	0.087	84.15

in coincidence net counts corresponding to the radioactivity of ^{3}H, with an R^2 value of 0.9999.

Table 10 shows the achievable MDA calculated for different measurement times based on the detection efficiency (2.65E−03 ± 7.78E−05 % with a 95 % confidence level, k = 2) for ^{3}H derived from the experiments. The uncertainty of MDA is the combined uncertainty of the background count, sample mass, and detection efficiency. To ensure conservative MDA results, the highest values are considered, given the uncertainties.

3.5. Monitoring of uncontrolled emergency radiological release situation

In underwater environments, uncontrolled emergency radiological releases require a prompt response to ensure environmental and public radiation safety and to prevent the spread of radiological contamination. Traditional sample-based environmental radiation monitoring has set sampling intervals and requires considerable time for pre-treatment and measurement. Generally, in environmental radiation monitoring, ^{3}H is measured using LSC after a distillation process and the addition of a scintillation cocktail. This process, including pre-treatment and dark adaptation for LSC measurement, requires 2–3 days [19]. For ^{90}Sr measurement, the commonly used method is fuming nitric acid method for Sr-separation, which, including the time for milking ^{90}Y, takes over

Table 12
Plastic scintillators based detection part detection efficiency results for ^{3}H.

	^{3}H		
Radioactivity of sample [Bq]	1.77E+04 ± 266	2.65E+04 ± 398	3.54E+04 ± 531
Background coincidence counts	587,679 ± 767		
^{3}H coincidence net counts	627,998 ± 792	648,521 ± 805	668,656 ± 818
Measurement time [s]	86,400		
^{3}H coincidence net count rate [cps]	0.467 ± 0.013	0.704 ± 0.013	0.937 ± 0.013
Detection efficiency [%]	2.64E−03 ± 8.22E−05	2.66E−03 ± 6.28E−05	2.65E−03 ± 5.40E−05

Table 11
Detection efficiency results of KCl according to measurement time.

	Sample 1	Sample 2	Sample 3	Sample 4	Sample 5	Sample 6
Radioactivity [Bq]	29.57 ± 0.30	59.13 ± 0.59	88.70 ± 0.89	118.27 ± 1.18	147.83 ± 1.48	236.53 ± 2.37
Measurement time [s]	3,600					
Coincidence net count rate [cps]	0.46 ± 0.07	0.92 ± 0.07	1.38 ± 0.07	1.85 ± 0.07	2.32 ± 0.07	3.69 ± 0.07
Detection efficiency [%]	1.565 ± 0.223	1.562 ± 0.112	1.561 ± 0.078	1.568 ± 0.060	1.567 ± 0.050	1.560 ± 0.034

two weeks for pre-treatment alone [19]. Unlike traditional sample-based environmental radiation monitoring systems, which consume significant time from sampling to pre-treatment and measurement, the continuous beta monitoring system in this study can monitor emergency radiological releases in underwater environments on-site without pre-treatment.

In Korea, according to the Enforcement Rules on Physical Protection and Radiological Emergency, there are regulations on the restriction of food intake and the control of the distribution or consumption of food, beverages, and agricultural, livestock, and marine products in areas affected by radiological emergencies [20]. For water, the criteria for restricting intake, distribution, or consumption are 100 Bq/L for ^{90}Sr and 100 kBq/L for ^{3}H [21,22]. According to Table 10, the MDA for ^{90}Sr and ^{3}H subject to the Enforcement Rules on Physical Protection and Radiological Emergency in Korea can be achieved in approximately 20 min of sample and background counting time, which depends on measurement time.

Moreover, at the initial state of an emergency release, ^{90}Sr will decay into ^{90}Y as time elapses since it is released until secular equilibrium is reached, where the activity of ^{90}Y is related to that of ^{90}Sr as expressed in Equation (5) [23].

$$A_Y(t) = \frac{A_{Sr}(t)\lambda_Y}{\lambda_Y - \lambda_{Sr}}\left(1 - \frac{e^{-\lambda_Y t}}{e^{-\lambda_{Sr} t}}\right) \tag{5}$$

where.

$A_Y(t)$ and $A_{Sr}(t)$: activity of ^{90}Y and ^{90}Sr over time (t),

λ_Y and λ_{Sr}: decay constant of ^{90}Sr and ^{90}Y.

Therefore, ^{90}Sr activity can be obtained from the total activity including both ^{90}Sr and ^{90}Y using Equation (6), where the measurement activity includes the contribution from both nuclides.

$$A_{Sr}(t) = \frac{A(t)}{1 + \frac{\lambda_Y}{\lambda_Y - \lambda_{Sr}}\left(1 - \frac{e^{-\lambda_Y t}}{e^{-\lambda_{Sr} t}}\right)} \cong \frac{A(t)}{2 - \frac{e^{-\lambda_Y t}}{e^{-\lambda_{Sr} t}}}, (\lambda_{Sr} \ll \lambda_Y) \tag{6}$$

where.

$A(t)$: total activity ($A_{Sr}(t) + A_Y(t)$).

4. Conclusion

A continuous beta monitoring system utilizing an integrated beta and gamma detection system was conceptually designed and evaluated for water samples from emergency radiological release situation. The system comprised a NaI(Tl) detector for gamma nuclides and two plastic scintillation detectors for beta nuclides. It effectively removed the influence of gamma radiation on the coincidence counts from the plastic scintillation detection part using those from the NaI(Tl) detector.

The system was assessed through detection experiments for beta nuclides ^{3}H and ^{90}Sr. The MDA of the system met the criteria for restricting intake, distribution, or consumption of 0.1 Bq/g for ^{90}Sr and 100 Bq/g for ^{3}H with a measurement time of 20 min.

This study demonstrated that accurate coincidence counts for beta nuclides, excluding gamma nuclides, could be obtained from the in-situ measurement, expecting the effective application to the initial monitoring of uncontrolled releases of water samples from nuclear facilities.

CRediT authorship contribution statement

Woo Nyun Choi: Writing – original draft, Supervision, Conceptualization. **Seungbin Yoon:** Writing – review & editing, Methodology, Data curation. **Hyeonmin Lee:** Software, Investigation, Formal analysis. **Hee Reyoung Kim:** Project administration.

Declaration of competing interest

The authors declare that they have no known competing financial interests or personal relationships that could have appeared to influence the work reported in this paper.The author is an Editorial Board Member/Editor-in-Chief/Associate Editor/Guest Editor for *[Journal name]* and was not involved in the editorial review or the decision to publish this article.

Acknowledgments

This work was supported by the Korea Institute of Energy Technology Evaluation and Planning and the Ministry of Trade, Industry & Energy of the Republic of Korea (grant no. 20214000000410).

References

[1] S. Richards, T. Frye, J. Shepherd, T. Nicholson, G. Kuzo, U. Shoop, S. Sakai, R. Allen, Liquid Radioactive Release Lessons Learned Task Force Final Report, Washington District of Columbia, 2006.
[2] Nuclear Energy Institute, Industry Ground Water Protection Initiative-Final Guidance Document 07–07, NEI, Washington District of Columbia, 2007.
[3] Nuclear Safety and Security Commission, Notice No. 2017–17, regulation on environmental radiological surveillance and environmental radiological impact assessment around nuclear facilities. Nuclear Safety and Security Commission, 2017.
[4] J.M. Lim, G.S. Choi, Y.H. Cho, The Annual Report on the Environmental Radiological Surveillance and Assessment Around the Korea Atomic Energy Research Institute (No. KAERI/RR4687/2021), Korea Atomic Energy Research Institute, 2021.
[5] W.N. Choi, U. Lee, J.W. Bae, H.R. Kim, Minimum detectable activity of plastic scintillator for in-situ beta measurement system in ground water, Nucl. Eng. Technol. 51 (2019) 1169–1175, https://doi.org/10.1016/j.net.2019.02.001.
[6] U. Lee, W.N. Choi, J.W. Bae, H.R. Kim, Fundamental approach to development of plastic scintillator system for in situ groundwater beta monitoring, Nucl. Eng. Technol. 51 (2019) 1828–1834, https://doi.org/10.1016/j.net.2019.05.006.
[7] X.B. Tang, J. Meng, P. Wang, Y. Cao, X. Huang, L.S. Wen, D. Chen, Simulated minimum detectable activity concentration (MDAC) for a real-time UAV airborne radioactivity monitoring system with HPGe and $LaBr_3$ detectors, Radiat. Meas. 85 (2016) 126–133, https://doi.org/10.1016/j.radmeas.2015.12.031.
[8] C. Gong, G. Zeng, L. Ge, X. Tang, C. Tan, Minimum detectable activity for NaI(Tl) airborne γ-ray spectrometry based on Monte Carlo simulation, Sci. China Technol. Sci. 57 (2014) 1840–1845, https://doi.org/10.1007/s11431-014-5553-x.
[9] G.F. Knoll, Radiation Detection and Measurement, John Wiley & Sons, 2010.
[10] D.S. SolidWorks, Solidworks. Version Solidworks, vol. 1, 2005.
[11] Ortec Inc., High voltage power supply operating and service manual. https://www.ortec-online.com/-/media/ametekortec/manuals/5/556-mnl.pdfModel556.
[12] Ortec Inc., Dual spectroscopy amplifier operating and service manual. https://www.ortec-online.com/-/media/ametekortec/manuals/8/855-mnl.pdfModel855.
[13] Ortec Inc., Timing single-channel analyzer operating and service manual. https://www.ortec-online.com/-/media/ametekortec/manuals/5/551-mnl.pdfModel551.
[14] Ortec Inc., Time-to-amplitude converter single-channel analyzer operating and service manual. https://www.ortec-online.com/-/media/ametekortec/manuals/5/567-mnl.pdfModel567.
[15] J.H. Ely, C.E. Aalseth, J.I. McIntyre, Novel beta-gamma coincidence measurements using phoswich detectors, J. Radioanal. Nucl. Chem. 263 (2005) 245–250, https://doi.org/10.1007/s10967-005-0044-y.
[16] Ortec Inc., EASY-MCA-2KTM digital gamma-ray spectrometer User's manual. https://www.ortec-online.com/-/media/ametekortec/manuals/e/easy-mca-mnl.pdf.
[17] W. Sohn, G.B. Lee, Y.H. Yang, Review of contamination and monitoring of on-site groundwater at foreign nuclear power plants due to unplanned release, J. Radiat. Prot. 38 (2013) 124–131, https://doi.org/10.14407/jrp.2013.38.2.124.
[18] Hanyang University, Monitoring and Survey of Environmental Radiation in Seoul-Kyungki Districts (No. KINS/HR-081, vol. 9, Korea Institute of Nuclear Safety, 2001.
[19] G.S. Choi, H.R. Kim, W.R. Lee, G.H. Jeong, M.J. Kang, Y.H. Cho, S.D. Choi, H. K. Park, D.W. Park, C.W. Lee, The Procedure for Investigating the Radiation Environment Around the KAERI (No. KAERI/TR-4102/2010), Korea Atomic Energy Research Institute, 2010.
[20] Nuclear Safety and Security Commission, Ordinance of the prime minister No. 1952, enforcement Rules on physical protection and radiological emergency. Nuclear Safety and Security Commission, 2024.
[21] Nuclear Safety and Security Commission, Ordinance of the prime minister No. 1952, attached form 4 of enforcement Rules on physical protection and radiological emergency. Nuclear Safety and Security Commission, 2024.
[22] Nuclear Safety and Security Commission, Ordinance of the prime minister No. 1952, attached form 5 of enforcement Rules on physical protection and radiological emergency. Nuclear Safety and Security Commission, 2024.
[23] R.D. Evans, The Atomic Nucleus, vol. 582, McGraw-Hill, New York, 1955.